TECHNICAL ARTICLE

Structural characterization of caffeine–oxalic acid co-crystals from the powder diffraction pattern at the SPring-8 BL02B2 beamline

Kunihisa Sugimoto,[1,2,a)] Shogo Kawaguchi,[1] and Michitaka Takemoto[1]

[1]*Research and Utilization Division, Japan Synchrotron Radiation Research Institute (JASRI), 1-1-1 Koto, Sayo-cho, Sayo-gun, Hyogo 789-5198, Japan*

[2]*Department of Chemistry, Kobe University, 1-1 Rokkodai-cho, Nada-ku, Kobe 657-8501, Japan*

In this work, we developed an X-ray powder diffractometer system equipped with six solid-state detectors and used it to perform *ab initio* structure determination from the powder diffraction pattern data obtained for a caffeine–oxalic acid co-crystal. The crystal structure obtained from the powder diffraction data was consistent with the previously solved single-crystal structure (Trask reference), although slightly larger (by about 2%). The co-crystallization of pharmaceutically active molecules can modulate their physical properties such as solubility, stability, and bioavailability. For the investigation of pharmaceutical complexes, the ability to visualize molecular interactions such as hydrogen bonding would be very helpful toward understanding their physical properties. Given the rate at which the high-throughput screening of pharmaceutical complexes has grown, an analogous high-volume, high-resolution X-ray powder diffraction technique with high-throughput data collection ability would be useful. We also solved the crystal structures of an inorganic complex and metal organic framework, zinc acetate dihydrate and CPL-1, in order to demonstrate the performance of our new diffractometer system. © 2017 International Centre for Diffraction Data.
[doi:10.1017/S088571561700032X]

I. INTRODUCTION

The co-crystallization of pharmaceutically active molecules represents a viable means of enhancing the physical properties of a drug substance (Childs *et al*., 2004; Trask *et al*., 2005). Co-crystals are increasingly being considered in order to address the solubility, bioavailability, and/or other physical or chemical deficiencies of a given active pharmaceutical ingredient, because it is unnecessary to change the molecular structure of the original pharmaceutical species, even if its physical properties would otherwise be unsuitable for the final product. To elucidate the crystal structures of co-crystals, single X-ray crystal structure analysis is better than powder diffraction. However, in many cases, suitable X-ray quality crystals of the appropriate size cannot be produced, as co-crystalline materials are typically synthesized using slurry and co-grinding techniques. Recently, the high-throughput screening of pharmaceutical complexes has attracted attention as a means to select target proteins and/or molecules from a huge number of active complexes. This technique can identify suitable pharmaceutical complexes that will interact well with target molecules through an automated system. However, to rapidly screen these complexes by X-ray powder diffraction (XRPD) with this approach, the diffractometer requires not only high resolution but also high-throughput data collection. For high-throughput screening using high-resolution XRPD data, we selected a micro-strip solid-state detector, because it can result in superior data quality while allowing for fast data acquisition, and simple, maintenance-free operation. In this work, we developed a diffractometer that was equipped with six silicon micro-strip photon-counting detectors, which we applied to the *ab initio* structure determination of caffeine–oxalic acid co-crystals from their powder diffraction pattern. The performance of the proposed system was demonstrated by using it to solve the crystal structures of an inorganic complex and metal organic framework, zinc acetate dihydrate and $[\{Cu_2(pzdc)_2(pyz)\}_n]$ (pzdc = pyrazine-2,3-dicarboxylate; pyz = pyrazine) (CPL-1).

II. EXPERIMENTAL

A. Sample preparation

All chemicals were obtained from Sigma-Aldrich Co., Ltd. and used as received. For the caffeine–oxalic acid co-crystals, caffeine (98.2 mg; 0.5 mmol) and oxalic acid (22.5 mg; 0.25 mmol) were dissolved in acetonitrile (10 ml) by heating at reflux for 30 min. The solution was concentrated *in vacuo* until precipitation commenced. Crystals were isolated by filtration. Small amounts of gently ground zinc acetate dihydrate were used in a glass capillary having a diameter of 0.5 mm. A powder sample of CPL-1 was prepared according to a previously reported method (Kondo *et al*., 1999).

B. Data collection

High-resolution powder diffraction data were collected at room temperature, at the BL02B2 beamline at the SPring-8

---

a)Author to whom correspondence should be addressed. Electronic mail: ksugimoto@spring8.or.jp
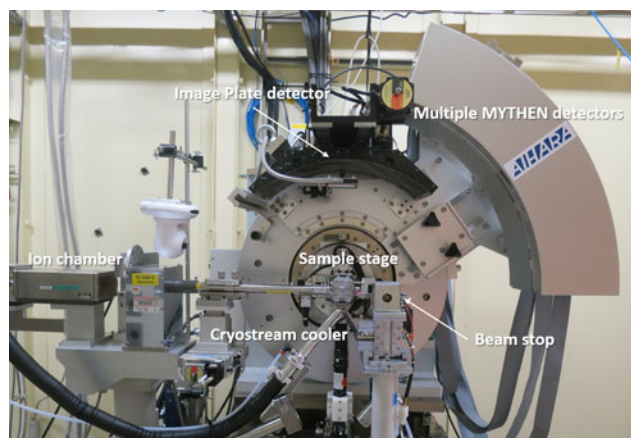
Figure 1. (Color online) Photograph of the diffractometer at BL02B2/SPring-8.

TABLE I. Feature of the developed X-ray powder diffractometer system.at BL02B2/SPring-8.

Diffractometer	
Diffraction geometry	Debye–Scherrer geometry
Sample-to-detector	477.46 mm
Detector	One dimensional type (Mythen)
Sensor thickness	1000 μm
Energy range	5–40 keV
Dynamic range	24 bits
Quantum efficiency	15 keV: 90%, 25 keV: 39%, 35 keV: 16%
Maximal count rate per channel	>1 × 10^6 photon s^{-1}
Frame rate	>17 fps
Dimensions of one module	64 × 8 mm^2
Number of channel	1280
Dimensions of one channel	0.05 × 8 mm^2
Receiving slit dimensions	2.5 × 8 mm^2
Minimum 2θ step	0.006°
2θ coverage of one detector module	7.63°

synchrotron radiation facility (Hyogo, Japan). Synchrotron radiation X-ray wavelengths of 0.998 636(4) Å for caffeine–oxalic acid co-crystals, 0.800 241(1) Å for zinc acetate dihydrate, and 0.800 283(2) Å for CPL-1 were selected using a double Si(111) crystal monochromator; X-ray wavelength calibration was performed with the standard reference material, CeO$_2$ (NIST 674b). The diffractometer was equipped with six MYTHEN silicon micro-strip photon-counting detectors (Dectris Ltd., Baden, Switzerland), and measurements were performed in the transmission geometry. A photograph of the assembled diffractometer and multiple MYTHEN detectors is shown in Figure 1. The distance between the sample and the detector was 477.46 mm, and the interval of the detector module was 12.5°. The sensitive area of one module was 64 × 8 mm^2, and the long side was set parallel to the 2θ direction. To reduce the effect of axial divergence substantially, the receiving slit (2.5 × 8 mm^2) was set in the front of the sensitive area of all modules. The 2θ coverage of one detector module was 7.63°, and the angular resolution was approximately 0.006° per channel. The 2θ angular range spanned from 2.00° to 78.21° for this detector arrangement. Continuous powder diffraction is usually allows us to combine data at two 2θ positions in order to fill the gaps between the detector modules (double-step mode). The detector arrangement described herein is similar to that at the BL15XU beamline at SPring-8 (Katsuya et al., 2016), which can simultaneously record data over the 2θ angular range from 2.00° to 38.10° in a "one-shot" measurement (single-step mode). The single-step mode is well suited for experiments that are time-resolved or conducted in operando. In this study, however, we chose the double-step mode because ab initio crystal structure determination from powder diffraction data would favor a wide 2θ range over the total data collection time. Table I summarizes the features of the developed X-ray powder diffractometer system.

For the powder XRPD experiments, hand-ground specimens of the caffeine–oxalic acid co-crystals, zinc acetate dihydrate, and CPL-1 were sealed in glass capillaries of 0.5 mm diameter. The sample was heated under reduced pressure, so that water molecules from the channels the CPL-1 structure could be removed and oxygen gas molecules could be adsorbed into the channels. After dehydration, the temperature was controlled at 95 K under oxygen gas atmosphere. The specimens were rotated during measurement for better particle

statistics. The lowest-angle diffraction peaks had a full-width-at-half-maximum (FWHM) of 0.037° (2θ) for the caffeine–oxalic acid co-crystals, 0.040° (2θ) for zinc acetate dihydrate, and 0.031° (2θ) for CPL-1; these values are significantly broader than the resolution of the spectrometer at this wavelength. The data for the caffeine–oxalic acid co-crystals were collected for 5 min at each position in the double-step mode from 2.094° to 78.216° (2θ).

C. Structure solution and refinement

Our goal was to demonstrate ab initio crystal structure determination from the powder pattern data collected at the BL02B2 with multiple MYTHEN detectors. The single-crystal structure of the co-crystal consisting of caffeine and oxalic acid (2:1) was reported by Trask et al. (2005). However, pharmaceutical complexes are usually prepared as microcrystalline powders, and suitable X-ray quality crystals of the appropriate size for single-crystal structural analysis cannot be produced on the production line. Therefore, it is worth demonstrating the ab initio determination of the crystal structure from the powder diffraction pattern, even if the crystal structure is known. Further, in order to demonstrate the performance of the new X-ray powder diffractometer system, the crystal structures of two other compounds, zinc acetate dihydrate and CPL-1, were solved from the powder diffraction patterns.

The structure of the co-crystal consisting of caffeine and oxalic acid was solved from the powder diffraction data using EXPO2014 software (Altomare et al., 2013). Indexing of the powder diffraction pattern of the co-crystal specimen was successfully achieved using the program N-TREOR09 after peak searching (Altomare et al., 2009). The space group of the caffeine–oxalic acid co-crystal could be unambiguously determined as $P2_1/a$ from the observed extinction rules (Altomare et al., 2004). The results of the indexing and space-group determination from the powder diffraction data were nearly identical to those of the single-crystal XRD experiment (Trask et al., 2005). Crystal structure determination was performed using direct methods. It was also possible to determine the partial crystal structure of the caffeine molecule in the co-crystal. The crystal structure of oxalic acid was determined
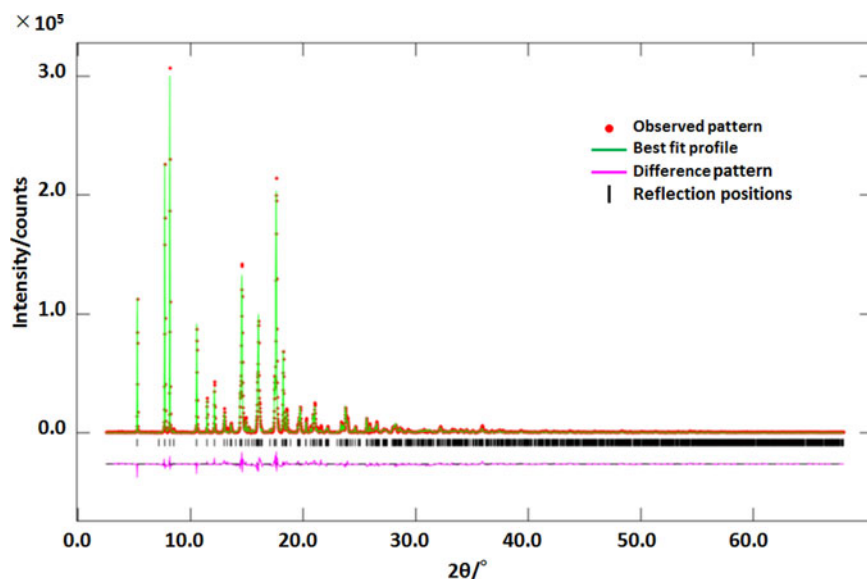
Figure 2. (Color online) Scattered X-ray intensity for caffeine–oxalic acid co-crystal as a function of diffraction angle 2θ. Shown are the observed pattern (red circle), the best Rietveld-fit profile in °(2θ) (bule line), the difference curve between observed and calculated profile (purple line), and the reflection marker.

using the Resolution Bias Modification procedure (Altomare *et al.*, 2008). The number of non-hydrogen atoms was 17 in the co-crystal of caffeine–oxalic acid. All hydrogen atoms were automatically added in ideal positions by the JAV Molecular Viewer in EXPO2014. A preliminary LeBail fit (LeBail *et al.*, 1988) was accomplished using the Rietveld refinement software GSAS (Larson and Von Dreele, 2000) and a pseudo-Voigt peak shape model in combination with a function that accounts for the asymmetry resulting from axial divergence (Thompson *et al.*, 1987; Finger *et al.*, 1994). The anisotropy of the FWHM was accounted for by the phenomenological strain model of Stephens (Stephens, 1999) as implemented in GSAS. In order to recognize the type of bonding between the carbon and oxygen atoms of the carboxylic group in oxalic acid, all atoms of oxalic acid without hydrogen were refined atomic coordinates, performing initial Rietveld refinement not using any constraints. The type of bounding was successfully determined by comparison with the ideal bond distance. Finally, in order to stabilize the Rietveld refinement, all refinements were carried out using restraints for bond lengths, angles, and planar groups based on ideal values using the "Soft constrains" function in the GSAS program. An overall atomic displacement parameter

TABLE II. Crystallographic data for caffeine–oxalic acid co-crystal solved by powder diffraction (this work) and single-crystal data.

Compound	Powder diffraction	Single-crystal data
Formula	$2(C_8H_{10}N_4O_2) \cdot C_2H_2O_4$	
Formula weight (g mol^{-1})	478.44	
Space group	$P2_1/a$	
Z	2	
a (Å)	16.0713(3)	16.0252(6)
b (Å)	14.8516(3)	14.7701(5)
c (Å)	4.4470(1)	4.4143(1)
β (°)	97.410(1)	99.399(1)
V (Å^3)	1052.57(1)	1030.81(2)
D-calc (g cm^{-3})	1.51	1.54
Wavelength (Å)	0.998 636(4)	–
R_p (%)[a]	3.62	–
R_{wp} (%))[a]	5.22	–
R–F^2 (%)[a]	14.23	–
Starting angle [°(2θ)]	2.094	–
Final angle [°(2θ)]	78.216	–
Step width [°(2θ)]	0.006	–
Exposure time (s)	300.0	–
Highest resolution for reflections (Å)	0.893	
Lowest resolution for reflections (Å)	10.865	
Number of reflections	1536	–
Number of variables	102	–
Reference	–	(Trask *et al.*, 2005)

[a]R_p, R_{wp}, and R–F^2 as defined in GSAS (Larson and Von Dreele, 2000).

TABLE III. Atomic coordinates and displacement parameters (Å^2) for caffeine–oxalic acid co-crystal solved from powder diffraction data.

| Atom	x	y	z	U_{eq}
C2	0.658 43(23)	0.140 75(22)	1.2034(9)	0.0667(9)
C3	0.789 23(30)	0.127 47(32)	1.5402(12)	0.0667(9)
C4	0.739 86(32)	0.408 17(26)	0.9259(14)	0.0667(9)
C5	0.5055(4)	0.4487(6)	0.0697(12)	0.0667(9)
C6	0.510 69(24)	0.257 54(24)	0.6065(8)	0.0667(9)
C7	0.473 15(31)	0.105 88(23)	0.8162(12)	0.0667(9)
C8	0.641 11(23)	0.281 41(22)	0.8814(8)	0.0667(9)
C9	0.609 47(22)	0.200 50(21)	0.9674(7)	0.0667(9)
C10	0.766 52(22)	0.267 19(24)	1.2231(9)	0.0667(9)
N2	0.737 51(21)	0.180 81(23)	1.3189(8)	0.0667(9)
N5	0.579 62(26)	0.319 81(21)	0.6529(8)	0.0667(9)
N6	0.528 15(22)	0.181 78(21)	0.8044(8)	0.0667(9)
N7	0.713 73(22)	0.318 00(23)	0.9966(9)	0.0667(9)
O2	0.4429(4)	0.4063(4)	0.1118(12)	0.0667(9)
O5	0.576 06(34)	0.4590(4)	0.2862(13)	0.0667(9)
O6	0.833 28(25)	0.300 69(30)	1.3326(10)	0.0667(9)
O7	0.629 53(31)	0.057 35(25)	1.2838(11)	0.0667(9)
H1	0.7510(6)	0.0957(26)	1.686(6)	0.0667(9)
H2	0.8342(21)	0.1694(8)	1.667(7)	0.0667(9)
H3	0.8200(22)	0.0775(19)	1.4253(24)	0.0667(9)
H4	0.7796(29)	0.4349(15)	1.113(6)	0.0667(9)
H5	0.6870(5)	0.4508(8)	0.878(12)	0.0667(9)
H6	0.7733(30)	0.4065(8)	0.736(8)	0.0667(9)
H7	0.459 16(30)	0.2656(5)	0.4638(10)	0.0667(9)
H8	0.4543(22)	0.1018(18)	1.0352(33)	0.0667(9)
H9	0.5052(9)	0.0466(6)	0.766(10)	0.0667(9)
H10	0.4197(15)	0.1146(15)	0.653(7)	0.0667(9)
H11	0.5917(26)	0.4011(9)	0.385(10)	0.0667(9)
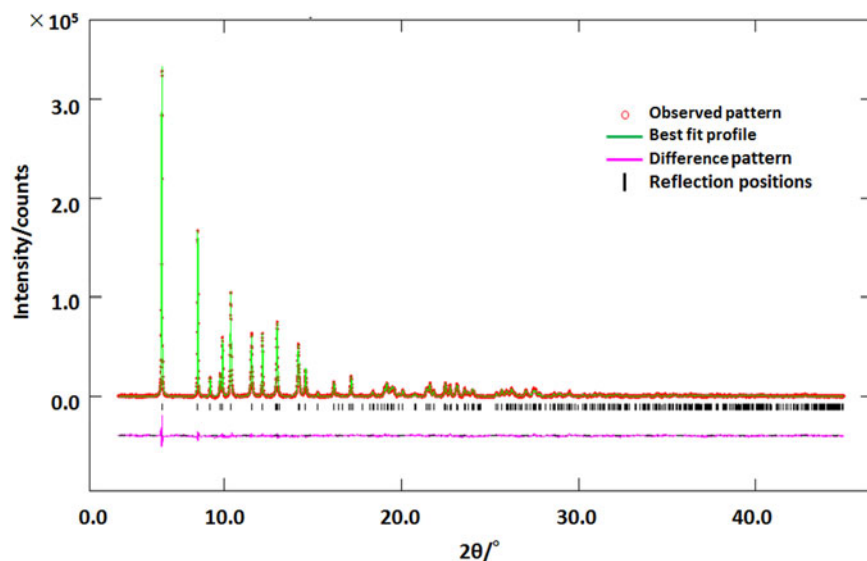
Figure 3. (Color online) Scattered X-ray intensity for zinc acetate dihydrate as a function of diffraction angle 2θ. The observed pattern (red circle), best Rietveld-fit profile in $°(2\theta)$ (blue line), difference curve between the observed and calculated profiles (purple line), and reflection marker are shown.
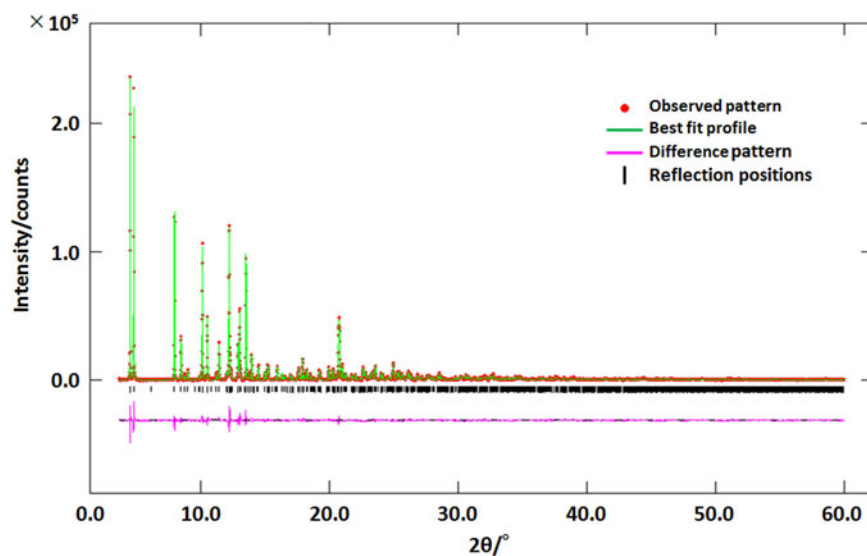

Figure 4. (Color online) Scattered X-ray intensity for CPL-1 as a function of diffraction angle 2θ. The observed pattern (red circle), best Rietveld-fit profile in $°(2\theta)$ (blue line), difference curve between the observed and calculated profiles (purple line), and reflection marker are shown.

for the caffeine–oxalic acid co-crystal was refined with the same parametric constraints. The final Rietveld plots are given in Figure 2 for the co-crystal consisting of caffeine and oxalic acid. Crystallographic data and agreement factors for the Rietveld refinements are listed in Table II, with the single-crystal data as reference. Atomic coordinates for the caffeine–oxalic acid co-crystal are listed in Table III.

For the crystal structure determination of zinc acetate dihydrate and CPL-1 from powder diffraction, the starting values of the lattice parameters, space groups, and atomic positions were taken from previously reported parameters (Ishioka *et al.*, 1997; Kitaura *et al.*, 2002) for Rietveld refinement (Rietveld, 1969). A preliminary LeBail fit (LeBail *et al.*, 1988) using the GSAS software (Larson and Von Dreele, 2000) and a pseudo-Voigt peak shape model in combination with a function that accounts for the asymmetry resulting from axial divergence (Thompson *et al.*, 1987; Finger *et al.*, 1994). The anisotropy of the FWHM was accounted for by the phenomenological strain model reported by Stephens (1999), as implemented in GSAS. In order to stabilize the Rietveld refinement for zinc acetate dihydrate and CPL-1,

all refinements were carried out using restraints for bond lengths, angles, and planar groups based on ideal values using the "Soft constrains" function in the GSAS program. All atomic displacement parameters for zinc acetate dihydrate and CPL-1 were refined freely without hydrogen atoms. The atomic displacement parameters of hydrogen atoms were constrained by more than 1.5 times for the methyl and carboxyl groups and 1.2 times for the aromatic group as compared to those for the carbon or oxygen atoms connected with the hydrogen atom. The final Rietveld plots are given in Figure 3 for zinc acetate dihydrate, with the single-crystal data as reference and Figure 4 for CPL-1. Crystallographic data and agreement factors of the Rietveld refinement are listed in Table IV for zinc acetate dihydrate and Table V for CPL-1. Atomic coordinates are listed in Table VI for zinc acetate dihydrate and Table VII for CPL-1.

III. RESULTS AND DISCUSSION

The structure of the co-crystal consisting of caffeine and oxalic acid is shown in Figure 5. The crystallographic cell

TABLE IV. Crystallographic data for zinc acetate dihydrate solved by powder diffraction (this work) and single-crystal data.

Compound	Powder diffraction	Single-crystal data
Formula	$Zn(CH_3COO)_2 \cdot 2H_2O$	
Formula weight (g mol^{-1})	219.50	
Space group	$C2/c$	
Z	4	
a (Å)	14.4044(4)	14.394(3)
b (Å)	5.334 87(9)	5.330(2)
c (Å)	10.967 67(22)	10.962(3)
β (°)	99.8824(16)	99.88(2)
V (Å^3)	830.31(5)	828.4(4)
D-calc (g cm^{-3})	1.76	1.76
Wavelength (Å)	0.800 241(1)	–
R_p (%)[a]	3.08	–
R_{wp} (%)[a]	3.97	–
R–F^2 (%)[a]	13.20	–
Starting angle [°(2θ)]	2.100	–
Final angle [°(2θ)]	78.210	–
Step width [°(2θ)]	0.006	–
Exposure time (s)	600	–
Highest resolution for reflections (Å)	1.046	–
Lowest resolution for reflections (Å)	7.095	–
Number of reflections	383	–
Number of variables	63	–
Reference	–	(Ishioka *et al.*, 1997)

[a]R_p, R_{wp}, and R–F^2 as defined in GSAS (Larson and Von Dreele, 2000).

volume solved from the powder sample is slightly larger (by about 2%) than that from the single-crystal data, because the powder sample of the caffeine–oxalic acid co-crystal was quickly crystallized from concentrated solution. The intermolecular interactions in the powder sample may therefore be slightly different from those in the single crystal. A detailed

TABLE V. Crystallographic data for CPL-1 adsorbed oxygen molecule at 95 K solved by powder diffraction.

Compound	CPL-1
Formula	$[Cu_2(C_6H_2O_4N_2)_2(C_4H_4N_2)] \cdot 2O_2$
Formula weight (g mol^{-1})	603.4
Space group	$P2_1/c$
Z	2
a (Å)	4.689 97(4)
b (Å)	20.4348(2)
c (Å)	10.9428(1)
β (°)	96.9398(6)
V (Å^3)	1041.06(2)
D-calc (g cm^{-3})	1.92
Wavelength (Å)	0.800 283(2)
R_p (%)[a]	2.91
R_{wp} (%)[a]	4.00
R–F^2 (%)[a]	11.79
Starting angle (°2θ)	2.1074
Final angle [°(2θ)]	78.217 39
Step width [°(2θ)]	0.006
Exposure time (s)	600
Highest resolution for reflections (Å)	0.8
Lowest resolution for reflections (Å)	10.217
Number of reflections	2120
Number of variables	74

[a]R_p, R_{wp}, and R–F^2 as defined in GSAS (Larson and Von Dreele, 2000).

TABLE VI. Atomic coordinates and displacement parameters (Å^2) for zinc acetate dihydrate at 300 K solved from powder diffraction data.

Atom	x	Y	z	U_{eq}
Zn1	0	0.1324(5)	0.25	0.0489(13)
O2	−0.0854(4)	−0.1164(18)	0.1500(5)	0.0616(29)
O3	0.1061(6)	0.4304(16)	0.2566(7)	0.062(4)
O4	0.0749(6)	0.2221(14)	0.0925(7)	0.078(4)
C5	0.1292(13)	0.3917(33)	0.1518(14)	0.135(8)
C6	0.1689(6)	0.5653(15)	0.0844(7)	0.107(5)
H7	−0.103(4)	−0.266(5)	0.1874(12)	0.080(4)
H8	−0.1097(35)	−0.084(5)	0.0654(15)	0.080(4)
H9	0.162(9)	0.516(14)	0.0001(27)	0.147(8)
H10	0.141(6)	0.725(4)	0.091(12)	0.147(8)
H11	0.2345(19)	0.578(20)	0.116(9)	0.147(8)

understanding of the bond distances and angles in the molecular structure solved from the powder specimen is not possible, because the structure was refined using restraints for those parameters. However, at a minimum, it is possible to discern the presence of intra- and intermolecular interactions, such as hydrogen bonding. The crystal packing structure of the caffeine–oxalic acid co-crystal is shown in Figure 6. The planarity of the oxalic acid molecule allows the adoption of a flat trimeric motif that can stack along the *a*-axis. In the context of the caffeine and oxalic acid co-crystal, the co-crystallization is guided by hydrogen bonding. Visualizing these kinds of molecular interactions is very useful for understanding the physical properties of pharmaceutical products, such as solubility and stability.

The structure of zinc acetate dihydrate is shown in Figure 7. Zinc acetate dihydrate has been used as medicine for treating Wilson's disease, with minimal side-effects. This compound is also used in other applications, such as wood preservation, polymers, dye mordants, and manufacture of ethylene acetate. The crystallographic cell volume solved

TABLE VII. Atomic coordinates and displacement parameters (Å^2) for CPL-1 adsorbed oxygen molecule at 95 K solved by powder diffraction.

| Atom	x	y	z	U_{eq}
CU1	0.6378(6)	0.163 70(9)	0.030 92(21)	0.015 28(24)
O2	0.8098(21)	0.1420(4)	0.2009(9)	0.015 28(24)
O3	1.0532(19)	0.1850(4)	0.3614(8)	0.015 28(24)
O4	1.4250(19)	0.3139(4)	0.3712(8)	0.015 28(24)
O5	1.0563(17)	0.3367(4)	0.4603(7)	0.015 28(24)
N6	0.6926(30)	0.2571(5)	0.0850(10)	0.015 28(24)
N7	0.9059(28)	0.3718(5)	0.2019(10)	0.015 28(24)
N8	0.5592(26)	0.0650(4)	−0.0040(12)	0.015 28(24)
C9	0.850(4)	0.2567(7)	0.1957(13)	0.015 28(24)
C10	0.9906(30)	0.3113(7)	0.2474(12)	0.015 28(24)
C11	0.7167(32)	0.3714(6)	0.0899(12)	0.015 28(24)
C12	0.6112(34)	0.3119(6)	0.0320(15)	0.015 28(24)
C13	0.8928(30)	0.1880(6)	0.2587(12)	0.015 28(24)
C14	1.1905(32)	0.3208(7)	0.3651(13)	0.015 28(24)
C15	0.4117(30)	0.0412(7)	0.0831(13)	0.015 28(24)
C16	0.6736(27)	0.0238(8)	−0.0875(12)	0.015 28(24)
O17	1.1711(26)	0.5084(5)	0.1400(10)	0.0772(30)
O18	0.9084(19)	0.5267(5)	0.1431(10)	0.0772(30)
H19	0.6876	0.4132	0.0408	0.015 31(28)
H20	0.4748	0.3149	−0.0479	0.015 31(28)
H21	0.3188	0.0697	0.1405	0.015 31(28)
H22	0.8031	0.0428	−0.1474	0.015 31(28)
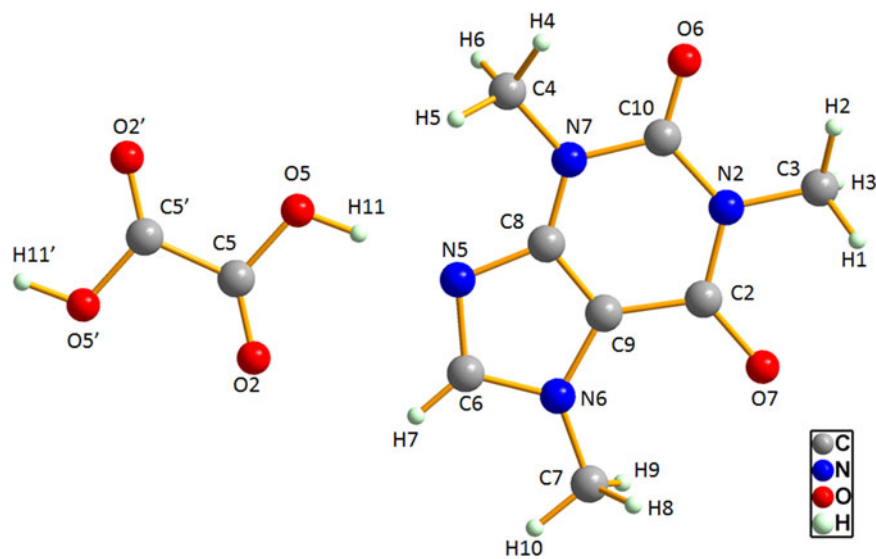
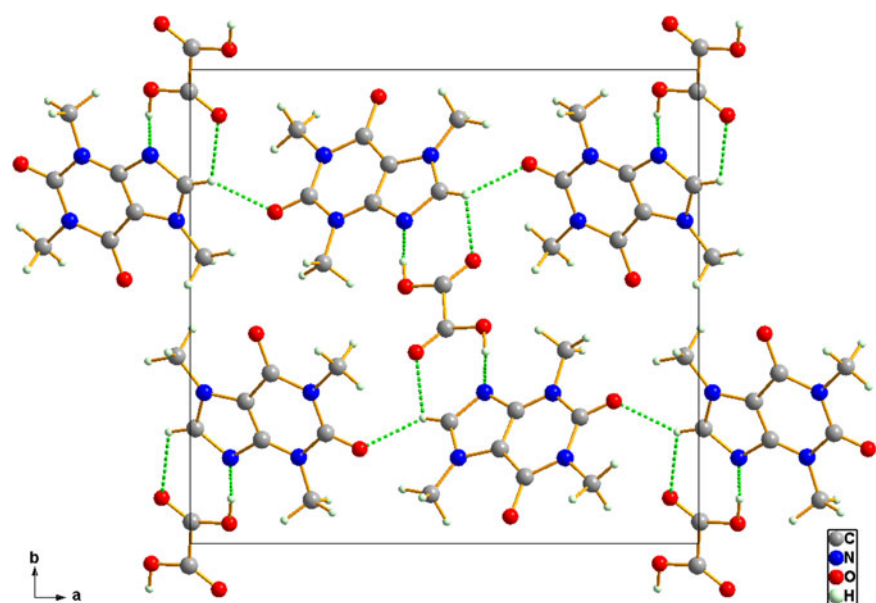Figure 5. (Color online) X-ray crystal structure of caffeine–oxalic acid co-crystal.

Figure 6. (Color online) X-ray crystal packing structures of caffeine–oxalic acid co-crystal along the *a*-axis, illustrating the hydrogen bond between caffeine and oxalic acid by green dashed line.

from the powder sample is almost the same as that from the single-crystal data. The six nearest neighbors of a zinc atom are four oxygen atoms and two water molecules, which form a distorted octahedron around the zinc atom. The formula units are linked by hydrogen bonds to form two-dimensional (2D) sheets (Figure 8). The crystal packing of zinc acetate dihydrate solved from the powder diffraction data is almost the same as that from the single-crystal data. Therefore, there is no notable difference between the physical properties of zinc acetate dihydrate powder and single-crystal samples.

The metal organic framework with a pillared layer structure, CPL-1, can adsorb oxygen gas molecules in the nano-channel structure. The 2D sheet constructed by Cu(II) and pzdc are bridged by pyz to form a pillared layer structure. A 1D channel is formed between the 2D sheet along the *a* axis. The structure of CPL-1 is shown in Figure 9 after adsorption of oxygen gas molecules in the channels. According the reported crystal analysis of CPL-1, the adsorbed oxygen gas molecules at the center of the channel were visualized in an intelligent manner by combining the maximum entropy
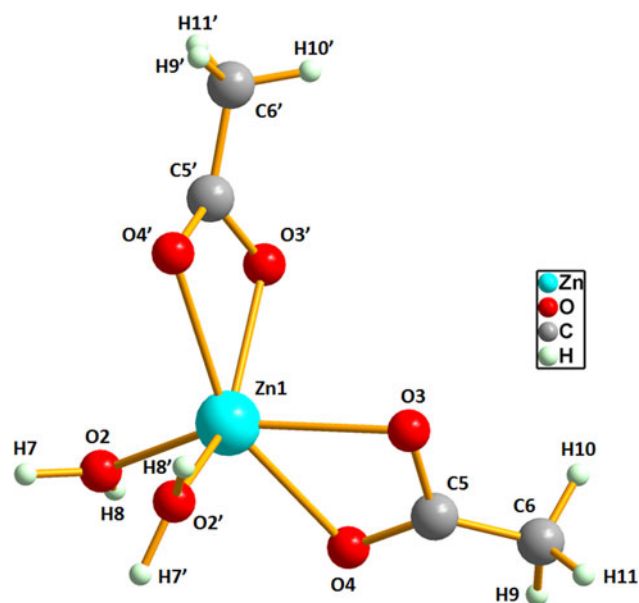

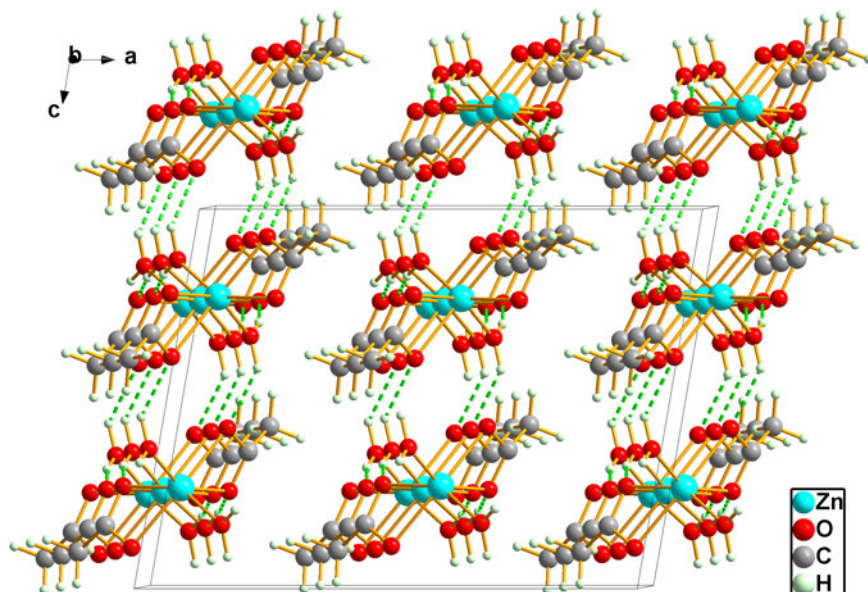Figure 7. (Color online) X-ray crystal structure of zinc acetate dihydrate.

Figure 8. (Color online) X-ray crystal packing structures of zinc acetate dihydrate along the *a*-axis, illustrating the hydrogen bond between neighboring molecules by green dashed line.
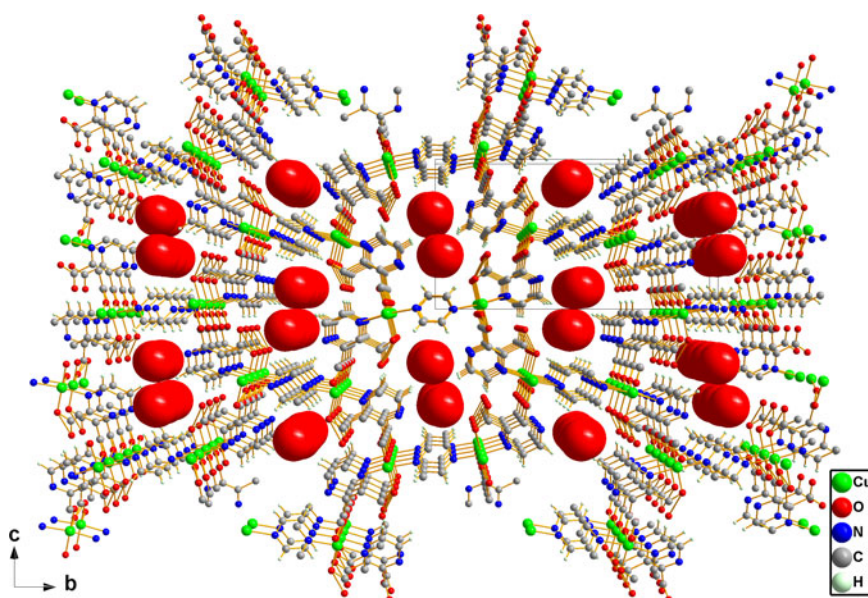

Figure 9. (Color online) Perspective view of the X-ray crystal packing structures of CPL-1 in central projection (camera distance 50 cm) down to the *a*-axis. The position of the oxygen gas molecules within the channels are presented by a space-filling model.

method and Rietveld refinement. However, it was possible to determine the charge density induced by the adsorbed oxygen molecules on the difference Fourier map from the present powder diffraction data during the general Rietveld refinement process. Thus, we demonstrated that the developed X-ray detector system could afford powder diffraction data with high accuracy.

We successfully developed a diffractometer with six silicon micro-strip photon-counting detectors. The quality of the powder diffraction pattern data was suitable for *ab initio* structure determination and Rietveld refinement. For a pharmaceutical complex, it is important to be able to determine the crystal structure from the powder diffraction pattern in order to reveal the sources of its physical properties. Currently, useful software for structure determination from powder diffraction data is freely or commercially available worldwide. We believe this developed diffractometer configuration will not only contribute to the analysis of pharmaceutical complexes,

including in high-throughput screens, but also allow for industrial investigations such as time-resolved experiments. In the near future, we will incorporate an auto-sampler into the diffractometer to increase throughput, so that the system can automatically switch specimens for continuous data collection.

SUPPLEMENTARY MATERIAL

To view supplementary material for this article, please visit https://doi.org/10.1017/S088571561700032X.

ACKNOWLEDGEMENTS

Altomare, A., Caliandro, R., Camalli, M., Cuocci, C., da Silva, I., Giacovazzo, C., Moliterni, A. G. G., and Spagna, R. (**2004**). "Space-group determination from powder diffraction data: a probabilistic approach," J. Appl. Crystallogr. **37**, 957–966.

Altomare, A., Cuocci, C., Giacovazzo, C., Moliterni, A., and Rizzi, R. (**2008**). "Correcting resolution bias in electron density maps of organic molecules derived by direct methods from powder data," J. Appl. Crystallogr. **41**, 592–599.

Altomare, A., Campi, G., Cuocci, C., Eriksson, L., Giacovazzo, C., Moliterni, A., Rizzi, R., and Werner, P.-E. (**2009**). "Advances in powder diffraction pattern indexing: N-TREOR09," J. Appl. Crystallogr. **42**, 768–775.

Altomare, A., Cuocci, C., Giacovazzo, C., Moliterni, A., Rizzi, R., Corriero, N., and Falcicchio, A. (**2013**). "EXPO2013: a kit of tools for phasing crystal structures from powder data," J. Appl. Crystallogr. **46**, 1231–1235.

Childs, S. L., Chyall, L. J., Dunlap, J. T., Smolenskaya, V. N., Stahly, B. C., and Stahly, G. P. (**2004**). "crystal engineering approach to forming cocrystals of amine hydrochlorides with organic acids. molecular complexes of fluoxetine hydrochloride with benzoic succinic, and fumaric acids," J. Am. Chem. Soc. **126**, 13335–13342.

Finger, L. W., Cox, D. E., and Jephcoat, A. P. (**1994**). "A correction for powder diffraction peak asymmetry due to axial divergence," J. Appl. Crystallogr. **27**, 892–900.

Ishioka, T., Murata, A., Kitagawa, Y., and Nakamura, K. T. (**1997**). "Zinc(II) acetate dihydrate," Acta Crystallogr. **C53**, 1029–1031.

Katsuya, Y., Song, C., Masahiko Tanaka, M., Ito, K., Kubo, Y., and Sakata, O. (**2016**). "Note: an X-ray powder diffractometer with a wide scattering-angle range of 72° using asymmetrically positioned one-dimensional detectors," Rev. Sci. Instrum. **87**, 016106.

Kitaura, R., Kitagawa, S., Kubota, Y., Kobayashi, T. C., Kindo, K., Mita, Y., Matsuo, A., Kobayashi, M., Chang, H., Ozawa, T. C., Suzuki, M., Sakata, M., and Takata, M. (**2002**). "Formation of a one-dimensional array of oxygen in a microporous metal-organic solid," Science **298**, 2358–2361.

Kondo, M., Okubo, T., Asami, A., Noro, S., Yoshitomi, T., Kitagawa, S., Ishii, T., Matsuzaka, H., and Seki, K. (**1999**). "Rational synthesis of stable channel-like cavities with methane gas adsorption properties: $[\{Cu_2(pzdc)_2(L)\}_n]$ (pzdc = pyrazine-2,3- dicarboxylate; L = a Pillar Ligand)," Angew. Chem. Int. Ed. Engl. **38**, 140–143.

Larson, A. C. and Von Dreele, R. B. (**2000**). *General Structural Analysis System (GSAS)* (Los Alamos National Laboratory Report No. LAUR-86-748).

LeBail, A., Duroy, H., and Fourquet, J. L. (**1988**). "*Ab-initio* structure determination of $LiSbWO_6$ by X-ray powder diffraction," Mat. Res. Bull. **23**, 447–452.

Rietveld, H. M. (**1969**). "A profile refinement method for nuclear and magnetic structures," J. Appl. Crystallogr. **2**, 65–71.

Stephens, P. W. (**1999**). "Phenomenological model of anisotropic peak broadening in powder diffraction," J. Appl. Crystallogr. **32**, 281–289.

Thompson, P., Cox, D. E., and Hastings, J. B. (**1987**). "Rietveld refinement of Debye-Scherrer synchrotron X-ray data from Al_2O_3," J. Appl. Crystallogr. **20**, 79–83.

Trask, A. V., Motherwell, W. D. S., and Jones, W. (**2005**). "Pharmaceutical cocrystallization: engineering a remedy for caffeine hydrate," Cryst. Growth Des. **5**, 1013–1021.